Interface dynamics, pole trajectories, and cell size statistics

C. Almarcha,[1] B. Radisson,[1] E. Al Sarraf,[1] E. Villermaux,[1,2] B. Denet,[1] and J. Quinard[1]

[1]*Aix Marseille Université, CNRS, Centrale Marseille, IRPHE UMR 7342, 13384 Marseille, France*
[2]*Institut Universitaire de France, Paris, France*

We demonstrate the possibility to reproduce the experimental evolution of an interface, here a flame front, through the trajectory of a few poles whose position in the complex plane expresses the interface shape. These poles are analytical solutions of the Sivashinsky equation and they evolve according to an ordinary differential equation. The direct comparison with experimental flame fronts propagating in a quasi-two-dimensional configuration is made at the nonlinear but deterministic stages of the front dynamics, reproducing a cell creation and fusion process. At later times, when the front is sensitive to noise as in the Kardar-Parisi-Zhang equation, we demonstrate that the cell size distribution is still ruled by the pole attractive nature.

An interface is a thin out-of-equilibrium region separating a metastable bulk phase from a stable one. At this layer, phase transitions or reactions can occur [1–3], involving diverse fluxes with diverse lengths and timescales. A paradigmatic example is a flame front, a submillimeter interface that propagates into a mixture of reacting gas and transforms it into products. Through this thin layer, density, normal velocity, and temperature change by an order of magnitude due to the energy released by hundreds of competing exothermic chemical reactions. When this interface remains flat, its normal propagation velocity is constant and can be computed in a one-dimensional model taking into account the chemical reaction rates and the diffusivities of the species and temperature. However, interfaces suffer various instabilities and in general do not remain flat. Their evolution, sometimes modeled by partial differential equations (PDEs), is routinely studied by direct numerical simulations.

The corrugations of a flame can be induced by an external forcing, when it is propagating in turbulent flow [4]. In that case the flame is wrinkled by the underlying flow where it propagates. But flame wrinkling can also develop in the absence of forcing, due to the intrinsic Darrieus-Landau (DL) instability [5]. The increase of volume and normal velocity through the flame leads to this nonlocal hydrodynamical instability, which is not only encountered in the domain of combustion but also in ionizing waves in inertial confinement fusion or in thermonuclear process in white dwarfs to name a few [6,7]. A nonlinear PDE, the Michelson Sivashinsky (MS) equation [8], is supposed to reproduce the DL instability in flames and their evolution but the detailed comparison with real flame experiments is tricky and has been limited up to now to the saturation of a single wavelength [9]. When a moderate external forcing is acting on the flame as a source of noise, the MS equation can be extended to a forced MS equation (FMS) [10] whose structure is close to the Kardar-Parisi-Zhang (KPZ) equation [11], the simplest nonlinear Langevin equation for a local growth, extensively used to describe the interface growth by additive white noise [12]. They only differ by nonlocal instability term in FMS. Such extensions of the

KPZ equation (sometimes named HKPZ equation [13]) with the addition of nonlocal instability terms [14] can be obtained in the context of molecular beam epitaxy leading to Asaro-Tiller-Grinfeld elastic instability [15], for the displacement of fluids with different viscosities leading to a Saffman-Taylor instability, for solidification fronts under the Mullins-Sekerka instability, or for reactive infiltration in porous media [13]. In contrast, growing interfaces in nematic liquid crystals [16] and flameless paper combustion [17], do not possess a nonlocal instability term and satisfy KPZ equation scalings, at least at sufficiently large scale [18].

Flame fronts are classically described by fractal dimensions [19,20], wrinkling factors [21], and various scalings in experiments [4] or numerical simulations [22–25]. Here we show that the deterministic nonlinear dynamics of a whole flame can be recovered using the MS equation with a very good accuracy. Moreover, since pole solutions to the MS equation exist [26], we demonstrate that experimental flame shapes can be described analytically by the trajectory of a few poles evolving in the complex plane according to a few coupled ordinary differential equations (ODEs). In addition, we show that in the late time evolution, when the importance of noise cannot be neglected anymore and the direct comparison with deterministic pole trajectories fails, the geometrical statistical description of the flame is still ruled by the pole attraction natural dynamics.

The experimental facility consists of a Hele-Shaw cell [27–29]: two vertically oriented glass-ceramic plates, 0.5 m wide and 1.5 m high, separated by a 5-mm gap width, closed on the sides, opened at the top are continuously filled with a premixed propane-air mixture at the desired equivalence ratio until the flame is ignited at the top (Fig. 1). The evolution of the luminous flame front location is recorded using a high-speed camera (500 fps). Qualitative results in this two-dimensional geometry are presented in [30], and emphasize its interest compared to tube propagation [31]. An example of evolution in the course of time is reported in Fig. 2(a) for lean propane air flame at equivalence ratio 0.9. The field of view is 203 mm large, with 0.006 s between each frame showing
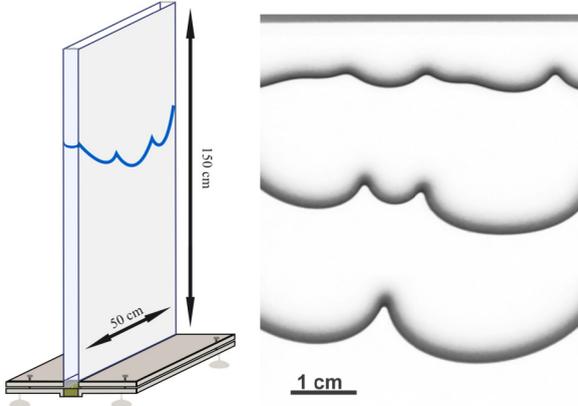
FIG. 1. Left: Sketch of the vertical Hele-Shaw cell. Right: Zoom on a lean propane-air flame front at different heights (inverted colors). The flame is initially anchored on the upper edge. When the upstream flow of reacting gas is stopped the flame moves downward and is destabilized.

an initial linear stage with growth of corrugations from an initially flat flame. Soon, cusps, local crests pointing toward burnt gases, grow and merge, thus coarsening the pattern. Eventually new cusps are formed in locally flat zones.

Our first aim is to compare quantitatively this cusp dynamics to the integration of the MS equation. The latter accounts for the evolution of the position $\phi(x, t)$ of the flame front location along the (horizontal) axis x defined by its mean position. This equation was originally derived in the limit of long wavelengths and unburnt to burnt gas expansion ratios $\theta = \rho_u/\rho_b$ close to unity, and later extended to larger gas expansions [32] and nonpotential flows [33–35] while keeping the same functional structure. It writes as

$$\phi_t + \frac{u_A}{2}\phi_x^2 = 4\frac{\sigma_M}{k_c}\left(\frac{\phi_{xx}}{k_c} + I(\phi, x)\right), \quad (1)$$

where $I(\cdot, x)$ is a nonlocal operator corresponding to the multiplication by $|k|$ in Fourier space. It stands for the Darrieus-Landau instability coming from Euler's equations in a potential flow. The velocity u_A depends on the nature of the reactants and on θ while σ_M and k_c are, respectively, the maximum growth rate and the cutoff wavelength of the associated dispersion relation

$$\sigma = 4\frac{\sigma_M}{k_c}\left(|k| - \frac{k^2}{k_c}\right). \quad (2)$$

These two quantities are measured experimentally in the linear stage of the front destabilization. Starting from an initially flat flame front anchored on the upper border of the Hele-Shaw cell, we analyze by way of Fourier transform the successive records of the flame contour when it penetrates the Hele-Shaw cell, as soon as the fresh gas mixture intake flow is stopped. A plate with periodic ripples placed a few millimeters above the burner allows one to excite a specific mode. This original procedure gives access to the linear growth rate. An example for propane air mixture with equivalence ratio 0.9 is reported in Fig. 3 and is compared to the best fit of the dispersion relation (2). The growth rates obtained compare favorably with the few measured previously in tubes [36],
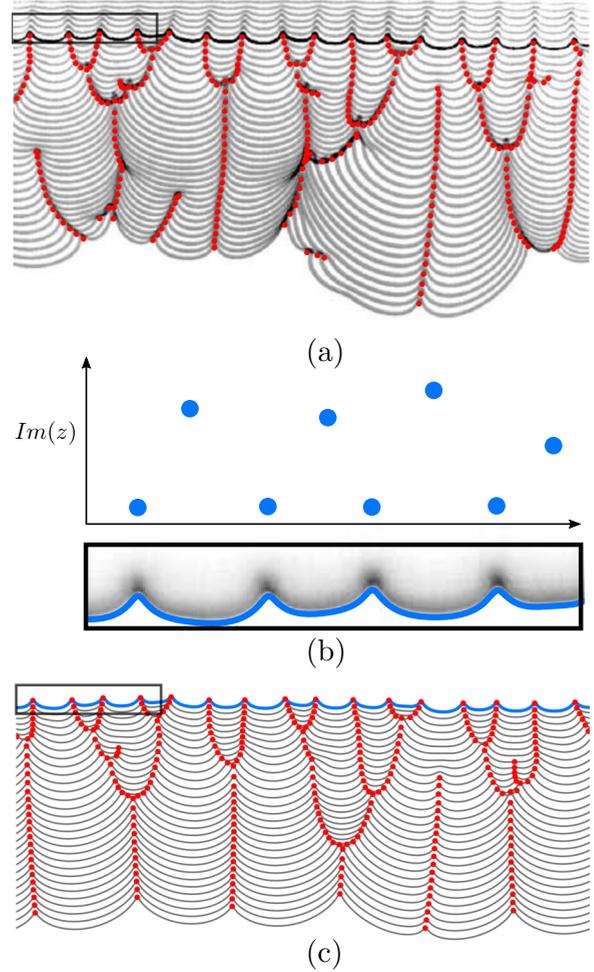

FIG. 2. (a) Downward propagation of an experimental propane-air flame front (equivalence ratio is 0.9). Red dots are placed on the cusps in order to track their trajectory. (b) Poles evaluated from the initial condition are represented by blue points. (c) Evolution of the pole solutions according to the system of ODEs (4).

where, however, only the growth rate of the most unstable mode was accessible, thus demonstrating the interest of the Hele-Shaw burner for the study of flame dynamics [27,37]. The MS equation (1) admits exact "pole-decomposable" periodic solutions [26] of the form

$$\phi = -A\sum_{n=1}^{2N}\ln\left[\sin\left(\frac{\pi(x - z_n)}{\Lambda}\right)\right], \quad (3)$$

where Λ is the width of the domain and $A = 8\sigma_M/u_A k_c^2$. The poles come in complex conjugate pairs, N being the number of poles with a positive imaginary part. Each pole z_n evolves according to the following coupled ODEs:

$$\dot{z}_n = \frac{4\sigma_M}{k_c}\left\{\sum_{p \neq n}^{2N}\frac{2\pi}{\Lambda k_c}\cot\frac{\pi(z_p - z_n)}{\Lambda} - i\,\mathrm{sgn}[\mathrm{Im}(z_n)]\right\}, \quad (4)$$

where $\mathrm{Im}(z_n)$ is the imaginary part of z_n.

In order to assess the validity of this system of equations, we used as an initial condition a frame (in bold) extracted
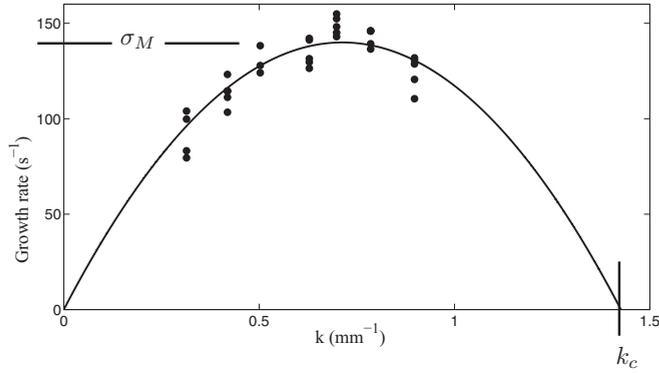
FIG. 3. Measurements of growth rate σ for lean propane air flame at equivalence ratio 0.9. The solid line is the least-square parabolic fit in accordance with the dispersion relation (2) exhibiting the maximum σ_M and cutting the horizontal axis at k_c.

from the experimental sequence reported in Fig. 2(a). By way of the Levenberg-Marquardt least-squares algorithm, we interpolated this experimental front presenting 16 cusps as the composition of 32 conjugate pole pairs. Their locations are represented by points over the frame in Fig. 2(b). Poles with a small imaginary part (vertical coordinate) induce visible cusps while the others are flattening the cells between the cusps. The pole trajectories (4) were integrated numerically in time [Fig. 2(c)]. The evolution of the simulated front exhibits cusp merging, and compares favorably with the evolution of the experimental one at the same instants of time. The remaining differences have their origin in the boundary conditions of the experimental front, the limited resolution of the camera, the flame front detection procedure, and the choice in the initial number of poles which, when integrating the ODEs (4), does not change in time. The creation of cells seen in Fig. 2(c) is thus entirely caused by poles present in the initial condition that get closer to the real axis, leading to visible new crests. At later times, the integration of (4) leads to the merging of all the cusps producing a unique cell, indicating that all the poles
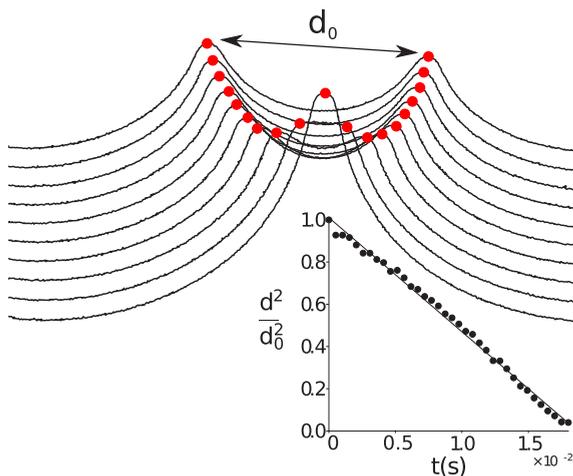

FIG. 4. Detail of a two-cusp fusion process in experiments. Field of view is 22 mm large. Inset: evolution of the squared distance between cusps in time (normalized by initial distance).
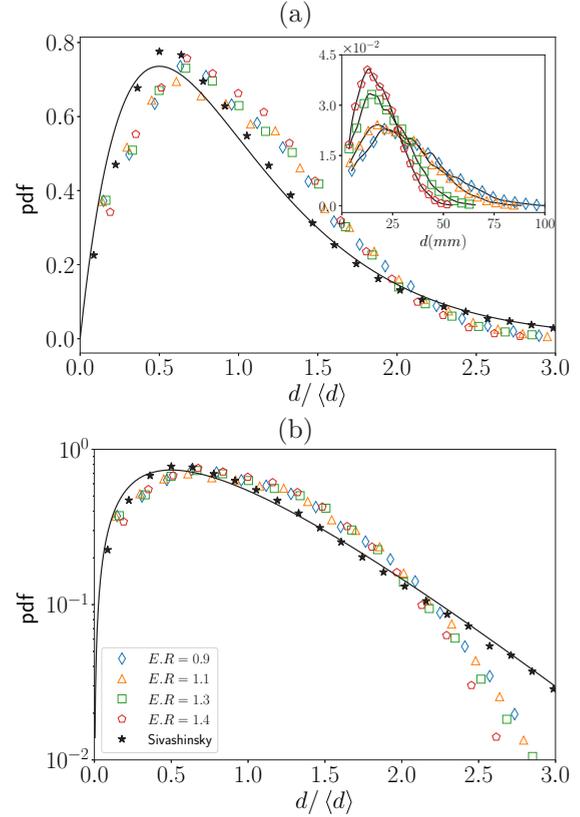

FIG. 5. Distribution of distances $p(\xi = d/\langle d \rangle)$ [and $p(d)$ in the inset] between successive cusps for propane-air flames with equivalence ratios between 0.9 and 1.4, in linear scale (a) and semilogarithmic scale (b). The result of the numerical integration of the MS equation is also reported. In the plots of the distribution of normalized distances ξ, the solid line is the gamma distribution with order $\nu = 2$.

are at the same abscissa. This is not what is happening in the experiment: new cusps separating new cells are appearing in the course of time [30] showing that the comparison with pole trajectories is limited in time if there is no addition of new poles. Sources of physical noise, for instance fluctuations in the upstream flow, are capable of creating these new poles [38], leading to a statistical steady state of the flame. To take into account the physical noise effects in numerical simulations, it is then possible to periodically introduce poles in the numerical simulation as proposed in [39], or to proceed to integration of the MS equation with the addition of a noise term introduced in the same way as in the KPZ equation. Another limitation of both the MS equation and of the pole description is that the front is single valued, which is not always the case in the experiment, as seen on the late frames of Fig. 2(a), an effect even more pronounced at a higher equivalence ratio.

However, we use the MS model and its pole solution to investigate important general aspects of the flame dynamics and of its geometrical features. In particular, we focus on the distribution of cell sizes (i.e., the distance d between two cusps). Considering two pairs of conjugate poles separated by a distance d sufficiently small for neglecting the interactions with other pairs of poles and in the limit of small imaginary

parts, Eq. (4) reduces to

$$\dot{d} \approx -2D \frac{\pi}{\Lambda} \cot \frac{\pi d}{\Lambda}, \tag{5}$$

where $D = 16\sigma_M/k_c^2$, whose solution at a short distance is singular as

$$d^2(t) \approx d_0{}^2 - 4Dt, \tag{6}$$

showing that the squared distance between two cusps initially separated by d_0 decreases linearly in time until fusion at $d_0{}^2/4D$. This is verified experimentally in Fig. 4. Cusp fusion means adjacent cells sizes addition [41], and if these additions are made at random, irrespective of the initial cell sizes at merging, then the distribution of their sizes $p(d)$ must be stable by self-convolution [40], and therefore of the gamma type [40,41]:

$$p(\xi = d/\langle d \rangle) = \frac{\nu^\nu}{\Gamma(\nu)} \xi^{\nu-1} e^{-\nu\xi}, \tag{7}$$

where ν depends on the microscopic dynamics producing the sizes d in Eq. (7). The aggregation dynamics in Eq. (6) is such that all cells initially smaller than the current average size $\langle d \rangle$ have a merging time smaller than the mean. The *incomplete convolution theory* [40] explains that this should occur for a critical size given by $2\langle d \rangle/\nu$, thus selecting the order $\nu = 2$. Experimental distributions are reported in Fig. 5(a) for propane-air mixtures at equivalence ratios between 0.9 and 1.4. After rescaling by the mean size $\langle d \rangle$, all distributions collapse, showing that the creation-fusion dynamics of the cells is universal, and is reasonably close to that obtained by numerical integration of the MS equation. Here for 200

unstable modes in the numerical domain, the round-off and truncation errors [42] create a numerical noise [38] that induces cusp creations and leads to a stationary distribution. When increasing the level of noise, the cusp creations increase [38] leading to smaller mean cell size, but we found that the normalized distribution remains the same, extremely close to the expected gamma of order $\nu = 2$. The experimental distributions present a more rapid falloff for very large cells. The source of this discrepancy may be in gravity (not present in the numerics) which limits the height and the width of the larger cells. This will be discussed in a forthcoming paper.

We have thus demonstrated that the rich dynamics of an interface can be represented by a single equation; in the present case, the MS equation which is a form of the KPZ equation where a nonlocal instability term is added or replaces the source of noise term. In that framework, the dynamics of the interface in the absence of noise amounts to computing the trajectories of only a few poles in the complex plane. This method, which can be extended to three-dimensional flames [43], provides insight into the local dynamics of the front exhibiting cells fusion, and into its statistical features in the presence of noise, namely, the cell size distribution. It is a major simplification effort whose interest is likely to expand beyond the domain of flame fronts, and may concern any physical phenomenon which presents a developing interface.

[1] Y. T. Fukai and K. A. Takeuchi, Phys. Rev. Lett. **119**, 030602 (2017).

[2] E. E. Ferrero, L. Foini, T. Giamarchi, Al. B. Kolton, and A. Rosso, Phys. Rev. Lett. **118**, 147208 (2017).

[3] P. Baba, L. Rongy, A. De Wit, M. J. B. Hauser, A. Toth, and D. Horvath, Phys. Rev. Lett. **121**, 024501 (2018).

[4] S. Chaudhuri, F. Wu, D. Zhu, and C. K. Law, Phys. Rev. Lett. **108**, 044503 (2012).

[5] L. Landau, Acta Physicochim. USSR **19**, 77 (1944).

[6] M. A. Liberman, *Introduction to Physics and Chemistry of Combustion* (Springer-Verlag, Berlin, Heidelberg, 2008).

[7] P. Clavin and G. Searby, *Combustion Waves and Fronts in Flows* (Cambridge University Press, Cambridge, UK, 2016).

[8] G. I. Sivashinsky, Acta Astronaut. **4**, 1177 (1977).

[9] G. Searby, J.-M. Truffaut, and G. Joulin, Phys. Fluids **13**, 3270 (2001).

[10] F. Creta, N. Fogla, and M. Matalon, Combust. Theor. Mod. **15**, 267 (2011).

[11] M. Kardar, G. Parisi, and Y.-C. Zhang, Phys. Rev. Lett. **56**, 889 (1986).

[12] J. De Nardis, P. Le Doussal, and K. A. Takeuchi, Phys. Rev. Lett. **118**, 125701 (2017).

[13] P. Kechagia, Y. C. Yortsos, and P. Lichtner, Phys. Rev. E **64**, 016315 (2001).

[14] M. Nicoli, R. Cuerno, and M. Castro, Phys. Rev. Lett. **102**, 256102 (2009).

[15] J. N. Aqua, A. Gouyé, A. Ronda, T. Frisch, and I. Berbezier, Phys. Rev. Lett. **110**, 096101 (2013).

[16] K. A. Takeuchi and M. Sano, Phys. Rev. Lett. **104**, 230601 (2010).

[17] J. Maunuksela, M. Myllys, O.-P. Kahkonen, J. Timonen, N. Provatas, M. J. Alava, and T. Ala-Nissila, Phys. Rev. Lett. **79**, 1515 (1997).

[18] M. Myllys, J. Maunuksela, M. J. Alava, T. Ala-Nissila, and J. Timonen, Phys. Rev. Lett. **84**, 1946 (2000).

[19] V. V. Bychkov and M. A. Liberman, Phys. Rev. Lett. **76**, 2814 (1996).

[20] R. Yu, X. S. Bai, and V. Bychkov, Phys. Rev. E **92**, 063028 (2015).

[21] J. Yanez and M. Kuznetsov, Phys. Lett. A **380**, 2549 (2016).

[22] O. Kupervasser, Z. Olami, and I. Procaccia, Phys. Rev. Lett. **76**, 146 (1996).

[23] M. A. Liberman, M. F. Ivanov, O. Peil, D. Valiev, and L.-E. Ericsson, Combust. Theory Modell. **7**, 653 (2003).

[24] D. Fernandez-Galisteo, V. N. Kurdyumov, and P. D. Ronney, Combust. Flame **190**, 133 (2018).

[25] S. Kadowaki,, Phys. Fluids **11**, 3426 (1999).

[26] O. Thual, U. Frisch, and M. Hénon, J. Phys. (France) **46**, 1485 (1985).

[27] G. Joulin and G. Sivashinsky, Combust. Sci. Technol. **98**, 11 (1994).

[28] J. Sharif, M. Abid, and P. D. Ronney, Premixed-gas flame propagation in Hele-Shaw cells, Technical Report, Spring Technical Meeting, Joint U.S. Sections, Combustion Institute (1999).

[29] J. Wongwiwat, J. Gross, and P. D. Ronney, Flame propagation in narrow channels at varying Lewis number, Proceedings of the 25th International Colloquium on the Dynamics of Explosions and Reactive Systems, Paper 258 (2015).

[30] C. Almarcha, J. Quinard, B. Denet, E. Al-Sarraf, J. M. Laugier, and E. Villermaux, Phys. Fluids **27**, 091110 (2015).

[31] C. Almarcha, B. Denet, and J. Quinard, Combust. Flame **162**, 1225 (2015).

[32] G. Joulin and P. Cambray, Combust. Sci. Technol. **81**, 243 (1992).

[33] G. I. Sivashinsky and P. Clavin, J. Phys. **48**, 193 (1987).

[34] K. A. Kazakov and M. A. Liberman, Phys. Rev. Lett. **88**, 064502 (2002).

[35] K. A. Kazakov, Phys. Rev. Lett. **94**, 094501 (2005).

[36] C. Clanet and G. Searby, Phys. Rev. Lett. **80**, 3867 (1998).

[37] S. H. Kang, H. G. Im, and S. W. Baek, Combust. Theory Modell. **7**, 343 (2010).

[38] Z. Olami, B. Galanti, O. Kupervasser, and I. Procaccia, Phys. Rev. E **55**, 2649 (1997).

[39] G. Joulin, Combust. Sci. Technol. **60**, 1 (1988).

[40] A. Vledouts, N. Vandenberghe, and E. Villermaux, Proc. R. Soc. London, Ser. A **471**, 20150678 (2015).

[41] E. Villermaux and C. Almarcha, Phys. Rev. Fluids **1**, 041902(R) (2016).

[42] V. Karlin, Math. Models Methods Appl. Sci. **14**, 1191 (2004).

[43] A. Patyal and M. Matalon, Combust. Flame **195**, 128 (2018).